JOURNAL OF PROTEOMICS 75 (2012) 4632–4646

Available online at www.sciencedirect.com

SciVerse ScienceDirect

www.elsevier.com/locate/jprot

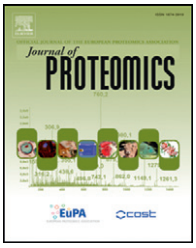

Proteomic profiling of ATM kinase proficient and deficient cell lines upon blockage of proteasome activity☆

Valeria Marzano[a,b], Simonetta Santini[c,d], Claudia Rossi[e,f], Mirco Zucchelli[e,f], Annamaria D'Alessandro[a,b], Carlo Marchetti[a,b], Michele Mingardi[c], Venturina Stagni[c,d], Daniela Barilà[c,d], Andrea Urbani[a,b,*]

[a]Proteomic and Metabonomic Laboratory, Fondazione Santa Lucia, 00143 Rome, Italy
[b]Department of Internal Medicine, University of Rome "Tor Vergata", 00133 Rome, Italy
[c]Laboratory of Cell Signaling, Fondazione Santa Lucia, 00143 Rome, Italy
[d]Department of Biology, University of Rome "Tor Vergata", 00133 Rome, Italy
[e]Centre of Study on Aging (CeSI), "G. d'Annunzio" University Foundation, 66100 Chieti, Italy
[f]Department of Biomedical Science, "G. d'Annunzio" University, 66100 Chieti-Pescara, Italy

ARTICLE INFO

Article history:
Received 28 October 2011
Accepted 16 May 2012
Available online 26 May 2012

Keywords:
ATM kinase
Proteasome
Shotgun
Carbohydrate metabolism

ABSTRACT

Ataxia Telangiectasia Mutated (ATM) protein kinase is a key effector in the modulation of the functionality of some important stress responses, including DNA damage and oxidative stress response, and its deficiency is the hallmark of Ataxia Telangiectasia (A-T), a rare genetic disorder. ATM modulates the activity of hundreds of target proteins, essential for the correct balance between proliferation and cell death. The aim of this study is to evaluate the phenotypic adaptation at the protein level both in basal condition and in presence of proteasome blockage in order to identify the molecules whose level and stability are modulated through ATM expression. We pursued a comparative analysis of ATM deficient and proficient lymphoblastoid cells by label-free shotgun proteomic experiments comparing the panel of proteins differentially expressed. Through a non-supervised comparative bioinformatic analysis these data provided an insight on the functional role of ATM deficiency in cellular carbohydrate metabolism's regulation. This hypothesis has been demonstrated by targeted metabolic fingerprint analysis SRM (Selected Reaction Monitoring) on specific thermodynamic checkpoints of glycolysis. This article is part of a Special Issue entitled: Translational Proteomics.

1. Introduction

Ataxia Telangiectasia (A-T) is an autosomal recessive disorder. The clinical hallmark of the disease is progressive neuromotor dysfunction resulting from gradual cerebellar cortical atrophy and Purkinje cells degeneration. Additional important features are telangiectasia in the eyes, thymic degeneration, immune deficiency, premature aging and higher predisposition to develop lymphomas and leukemia [1,2]. Moreover, A-T patients are highly sensitive to ionizing radiations (IR) [3]. A-T is linked to mutations of the ATM (Ataxia Telangiectasia Mutated) gene on both alleles, which ultimately impair the production of a functional ATM protein [4,5], a serine/threonine-PI3-kinase like protein originally identified as a central player of the DNA

☆ This article is part of a Special Issue entitled: Translational Proteomics.

* *Corresponding author at:* Proteomic and Metabonomic Laboratory, Fondazione Santa Lucia, Via del Fosso di Fiorano 64, 00143 Rome, Italy. Tel.: +39 06501703215; fax: +39 06501703332.
E-mail address: andrea.urbani@uniroma2.it (A. Urbani).

1874-3919/$ – see front matter © 2012 Elsevier B.V. All rights reserved.
doi:10.1016/j.jprot.2012.05.029

damage response (DDR) network [2]. ATM kinase mainly exerts its function through the phosphorylation of several protein substrates. These include proteins involved in cell cycle control, DNA repair and apoptosis, such as p53, Chk2, MRN complex, Rad51 and many more [3]. Following DNA damage, ATM molecule is (auto)phosphorylated on Ser 1981 and phosphorylation on this site has been proposed as a signature of an activation event [6]. ATM is activated mainly by DNA double strand breaks (DSBs), a cytotoxic lesion induced by IR, radiomimetic agents, such as neocarzinostatin (NCS), reactive oxygen species accompanying normal metabolism, and it triggers cell cycle arrest and DNA repair as well as, depending on the cellular context and on the severity of the damage, programmed cell death or apoptosis [7]. Increasing evidence suggests that the ubiquitin system plays a crucial role in the DDR providing a timed and coordinated degradation or relocalization or activation of regulatory proteins essential for the execution of the DDR [8]. In fact, cellular homeostasis maintenance and ability of adaptation to the environment depend on degradation of regulatory proteins. Furthermore, more recently non-degradative ubiquitylation of DNA repair proteins has been shown to play an essential role in the DDR. This post-translational modification of key DDR molecules provides direct and indirect routes to damage site recognition for DNA repair proteins [9]. Phosphorylation-dependent or independent ubiquitylation and deubiquitylation affect protein localization and pathway activation/inactivation and are signals regulating the multiple mechanisms allowing for DDR transient activity [10].

The ubiquitin–proteasome (Ub–P) system plays a key role in maintaining the integrity of cellular proteome and in protecting cells from protein damage. Accumulation of damaged proteins can interfere with normal cellular processes and may directly induce cell death. Under normal circumstances, ubiquitylation of proteins acts as a quality control mechanism, marking and destroying improperly manufactured proteins. Indeed upon cellular stresses such as metal and oxidants exposure or heat shock, there is a significant increase of ubiquitylated proteins level in the cell, and aberrations in this pathway are implicated in the pathogenesis of several diseases, including many neurodegenerative disorders [11,12].

In this scenario, it has been demonstrated that Ub–P is also induced in response to ATM kinase activation. NCS treatment endogenously increases ubiquitin conjugates in lymphoblastoid cells. A-T cells show an attenuated ability to mount the ubiquitylation response to stress, supporting a role of ATM in modulating the ubiquitylation machinery [13]. ATM modulates the activity of E3 ubiquitin ligases, affecting indirectly the stability of target proteins: for example the E3 ubiquitin ligases MDM2 and COP1 have been identified as ATM substrates and their ATM-dependent phosphorylation results in the inhibition of their enzymatic activity which in turn triggers p53 stabilization [14–16]. Recently, Stagni and colleagues have shown that ATM modulates the proteasome dependent down-regulation of c-FLIP therefore affecting death receptor induced apoptosis [17,18]. Furthermore it has been shown that ATM activity triggers NEMO ubiquitylation and NF-κB activation modulating the TNFα response [19]. A recent paper demonstrates how protein proteasome-mediated degradation is negatively affected in A-T cells due to the ATM impairment of ISG15 (an ubiquitin-like protein) pathway [20]. Importantly, proteomic approaches aimed to deciphering ATM substrates identified more than 700 proteins as novel ATM targets among which the Ub–P system is highly represented [21–23]. Moreover, these studies suggested that ATM may importantly contribute to several cellular functions beside DNA damage response. Indeed, DDR independent roles of ATM as cytoplasmic protein involved in different biochemical phenomena are starting to emerge linking ATM deficiency to increased oxidative stress, neurodegeneration, metabolic dysregulation and oncogenesis (reviewed in [24]). ATM participates in maintenance of cellular redox homeostasis by up-regulation of antioxidants, increasing production of reductive precursors and decreasing reactive oxygen species (ROS) production by mitochondria. Accordingly, the absence of a functional ATM results in a continuous state of oxidative stress causing adverse effects on particularly sensitive cells as neurons [25,26]. Moreover, an intrinsic up-regulation of ROS and mitochondria dysfunction are exhibited by ATM deficient lymphoblastoid cells [27] and Cheema and colleagues reported that ATM controls oxidative stress by regulating purine, pyrimidine and urea cycle pathways [28]. Interestingly, H_2O_2 dependent ATM Cys-2991 dimer formation was proposed as oxidation activation mechanism different from the classic Ser-1981 autophosphorylation occurring after the DBSs [29]. Other evidences supported ATM role in regulation of metabolic signaling pathways. ATM participates in insulin signaling through phosphorylation of eIF-4E-binding protein 1 [30] and glucose metabolism is affected by ATM activity as the levels of Insulin-like growth factor 1 receptor (IGFR1) are reduced in ATM-deficient cells [31] and translocation of the cell-surface Glucose transporter 4 (GLUT4) is regulated indirectly by ATM in response to insulin stimulation [32]. Moreover, a link between ATM and the pentose phosphate pathway has been provided [33] and ATM activity modulates metabolic syndrome [34,35].

Overall, these data confirm that ATM deficiency affects the cellular proteome composition resulting in multiple defective signaling pathways. Therefore, we developed a non-targeted proteomic investigation to analyze the profile of proteins whose levels change in response to ATM expression in order to elucidate the role of ATM in the control of protein quality and stability. To this aim, protein expression profiling was also assessed in the presence of the proteasome inhibitor MG132 to highlight those proteins whose expression is modulated by ATM most likely through the ubiquitin–proteasome system. Our investigation was pursued by the use of isotope-free shotgun proteomics approach that provides a relatively high-throughput assessment of changes in protein expression, which may act as a molecular remnant of ATM activity mechanism, and generates raw data for unsupervised data-mining of functional biological process. This approach allowed us to obtain an overview on the role of ATM in the modulation of the proteome, thereby offering a better understanding of its physiologic and pathologic implication.

2. Materials and methods

2.1. *Cell lines, antibodies and reagents*

L6pCDNA (L6), L6-Flag-ATM-wt (L6ATM), GM-03189 and HeLa cell lines were cultured as described previously [17,18,36].

Anti-Mono- and polyubiquitinylated conjugates (clone FK2) mAb was purchased from ENZO Life Sciences (Farmingdale, NY, USA). Anti-ATM (clone 2C1) mAb, anti-Lamin B (M-20) Ab, anti Matrin-3 (C-20) Ab, anti PGAM1 (6) mAb, anti-PGK1 (Y-12) Ab, anti PKM2 (H-59) Ab, anti-Stat1 (M-22) Ab and anti-T-Plastin (A-3) mAb were obtained from Santa Cruz Biotechnology (Santa Cruz, CA, USA). Anti-hnRNP F+H (1G11) mAb was obtained by Abcam (Cambridge, UK) and anti-GLRX1 (AF3119) Ab from R&D Systems Inc. (Minneapolis, MN, USA). Anti-β-Actin (clone AC-15) mAb and anti-α-Tubulin (Clone DM 1A) mAb were purchased from Sigma-Aldrich (Saint Louis, Missouri, USA). ShATM construct and its control (shSc) were described elsewhere [18]. The proteasome inhibitor Z-Leu–Leu–Leu-al (MG132), DMSO, Trizma base, Urea, CHAPS, Iodoacetamide (IAA), DTT, [Glu1]-Fibrinopeptide B, Ammonium acetate, Methanol, Ethanol, Acetone and standard compounds (glucose 6–phosphate, fructose 1,6-bisphosphate, glyceraldehyde 3–phosphate, pyruvate, lactate) were purchased from Sigma. Sequence grade trypsin was purchased from Promega (Madison, WI, USA). Water ultra-gradient, Acetonitrile ultra-gradient (ACN), TFA and Formic Acid (FA) were purchased by Romil (Cambridge, UK).

2.2. *Immunoblotting*

Protein extracts were obtained by lysing and sonicating cells in 6 M Urea, 100 mM Tris pH 7.5 and 0.5% CHAPS. Protein concentration was determined by the Bio-Rad Protein Assay (Bio-Rad Laboratories, Hercules, CA, USA). Equal amounts of proteins were resolved by 1-D-SDS-PAGE and blotted onto nitrocellulose membranes using a Hoefer SemiPhor semidry transfer unit (Amersham Biosciences, Uppsala, Sweden). Blots were incubated with the indicated primary antibodies, extensively washed and, after incubation with horseradish peroxidase (HRP)-labeled goat anti-mouse or anti-rabbit (Bio-Rad Laboratories) or bovine anti-goat Ab (Santa Cruz), developed with the ECL plus chemiluminescence's detection system (GE Healthcare, UK). The band intensities were quantified and normalized with those of α-Tubulin using the image analysis software: ImageQuant™ TL (GE Healthcare). Three independent experiments were done for each detected protein.

2.3. *Expression analysis by nLC-MS^E*

Proteins extracted from 10×10^6 L6 and L6ATM cells, treated with 10 μM MG132 or 1:1000 DMSO (control) for 2 hours, were quantified by Bio-Rad assay. Three different experiments were performed and four protein pools were obtained (L6, L6MG132, L6ATM and L6ATMMG132), collecting 50 μg of protein from each experiment. Proteins pools were precipitated adding a cold mix of Ethanol, Methanol and Acetone (ratio 2:1:1, v/v), and redissolved in 6 M Urea, 100 mM Tris pH 7.5. After reduction with 10 mM DTT and alkylation with 20 mM IAA, protein samples were digested 100:1 (w/w) with sequence grade trypsin at 37 °C overnight. The reaction was stopped by adding a final concentration of 0.1% TFA. Samples were diluted with 0.1% FA, 3% ACN at a concentration of 0.86 μg/μl, and 1.72 μg of protein digestion were loaded on column for peptide separation. Prior of loading, 100 fmol/μl *Saccharomyces cerevisiae* Enolase digestion (Waters, Milford, MA, USA) was added to samples as internal standard. Peptides were trapped on a 5 μm Symmetry C18 trapping column 180 μm × 20 mm (Waters) and separated using a 180 min RP gradient at 300 nl/min (3 to 40% ACN over 125 min) on a nanoACQUITY UPLC System (Waters), utilizing a 1.7 μm BEH 130 C18 NanoEase 75 μm × 25 cm nanoscale LC column (Waters). The lock mass ([Glu1]-Fibrinopeptide B, 500 fmol/μl) was delivered from the auxiliary pump of the UPLC System with a constant flow rate of 250 nl/min. The separated peptides were mass analyzed by a hybrid quadrupole orthogonal acceleration time-of-flight mass spectrometer (Q-Tof Premier, Waters Corp., Manchester, UK) directly coupled to the chromatographic system and programmed to step between low (4 eV) and high (15–40 eV) collision energies on the gas cell, using a scan time of 1.5 s per function over 50–1990 *m/z* (Expression analysis [37,38]). Three continuum LC-MS data for each pool were processed for qualitative and quantitative analysis using the software ProteinLynx Global Server (version 2.4, PLGS, Waters). Protein identifications were obtained with the embedded ion accounting algorithm of the software and searching a human database (UniProtKB/Swiss-Prot Protein Knowledgebase, release 2011_06 of 31-May-11 containing 529056 sequence entries; taxonomical restrictions: *Homo sapiens*, 20235 sequence entries) to which data from *S. cerevisiae* Enolase was appended. The search parameters were automatic tolerance for precursor ions and for product ions, minimum 3 fragment ions matched per peptide, minimum 7 fragment ions matched per protein, minimum 2 peptide matched per protein, 1 missed cleavage, carbamydomethylation of cysteine as fixed modification and oxidation of methionine as variable modification. The false positive rate estimated was under 4%, as previously described [39]. Quantitative analyses have been performed by data independent alternate scanning expression algorithm. Identified proteins were normalized against P00924 entry (*S. cerevisiae* Enolase) while the most reproducible peptides for retention time and intensity deriving from Enolase digestion (756.4604 *m/z*, 807.4302 *m/z*, 814.4923 *m/z*, 1159.6069 *m/z*, 1159.6069 *m/z*, 1755.9429 *m/z*) were used to normalize the EMRTs table, that is the list of peptide (Exact Masses paired to their Retention Times). In fact, the processing of the two mass spectrometric data functions, low energy and elevated energy, plus data of the reference lock mass, provides a time-aligned inventory of accurate mass-retention time components for both the low and elevated-energy (EMRT). The entire differentially expressed proteins data set was filtered by considering only those identifications from the alternate scanning LC-MS^E data with identified peptides exhibiting good replication rate (at least two out of three injections) and with a probability of upregulation (*p*-value) lower than 0.05 and upper than 0.95 associated to the relative protein fold change. Furthermore, the significance of regulation level was determined at 30% fold change, that is an average relative fold change between −0.30 and 0.30 on a natural log scale, which is typically 2–3 times higher than the estimated error on the intensity measurement (for more details see Supplementary Information Data S1).

2.4. *Bioinformatic analysis*

To identify Gene Ontology (GO) classes and biologically relevant molecular pathways from our large-scale data we have analyzed the proteomics dataset by using two different bioinformatic analysis tools endowed with a comprehensive knowledgebase,

such as Protein ANalysis Through Evolutionary Relationships (PANTHER) Classification System (version 7.0 http://www.pantherdb.org) [40] and Ingenuity Pathways Analysis (IPA; version 9.0, Ingenuity Systems, http://www.ingenuity.com). By PANTHER resource genes products can be categorized by their molecular functions and/or biological processes on the basis of published papers and by evolutionary relationships to predict function when interpreting experimental evidence is challenging. Ingenuity Pathways Analysis is a web-based application that enables mining, visualization and exploration of relevant functional associations significant to the experimental results. The analysis settings applied were: Reference set: Ingenuity Knowledge Base (Genes Only); Relationship to include: Direct and Indirect; Includes Endogenous Chemicals; Filter Summary: Consider all molecules and/or relationships. The most significant categories associated to the uploaded datasets were identified by calculating the related significance (p-value) statistically evaluated by the Fischer's exact test. The p-value measures the likelihood that the association between the genes/proteins in the datasets and each Canonical Pathway, Biological Function, etc., is not due to random chance alone identifying significant over-representation of molecules in association to a given process. We applied a p-value threshold of 0.05, limiting the false discovery rate (i.e., the expected fraction of false positives among significant functions) to less than 5%.

2.5. *Metabolomics analysis*

100 μL of a mixture of ethanol/water 80:20 were added to 20×10^6 cell pellets. Cells were sonicated for 20 min and then samples were centrifuged (25,000*g*, 4 °C, 20 min). Supernatants were analyzed by an LC-MS/MS system consisting of a Waters Alliance HT 2795 HPLC Separation Module coupled to a Waters Quattro Ultima Pt ESI tandem quadrupole mass spectrometer (Waters). The instrument was operated in negative electrospray ionization mode using MassLynx v. 4.0 software (Waters) and data processing was performed using QuanLynx software (Waters). For HPLC analysis, the Atlantis HILIC Silica 3 μm 2.1×150 mm column (Waters) was used. 25 μl of the extracted samples were injected onto the HPLC-MS/MS system. The mobile phase comprised a binary solvent system: ACN (solvent A) and water containing 50 mmol/l Ammonium acetate (solvent B). The initial solvent composition was 100% A. 100%A was maintained for 3 min; decreasing from the initial conditions to 50% A within 8.0 min, holding for 4 min before returning to the initial state at 12.0 min, allowing 4 min for column re-equilibration. The total run time was 16 min, injection-to-injection. The flow rate was 0.3 ml/min. The mass spectrometer ionization source settings were optimized for maximum precursor ion yields for each metabolite. This was achieved by infusing a 1 μg/ml methanolic solution of each individual compound. The following transitions were monitored for the metabolites of interest: glucose 6–phosphate (G 6–P) 258.80>96.80, cone 40 V and collision energy 13 eV; fructose 1,6–bisphosphate (F 1,6–P) 338.90>96.90, cone 40 V and collision energy 15 eV; glyceraldehyde 3–phosphate (G 3–P) 168.80>96.90, cone 40 V and collision energy 5 eV; pyruvate (P) 86.90>43.10, cone 40 V and collision energy 5 eV; lactate (L) 88.90>43.10, cone 40 V and collision energy 6 eV. The capillary voltage was 3.00 kV, source temperature was 100 °C, desolvation temperature was 400 °C, and the collision cell gas pressure was 3.5×10^{-3} mbar argon. The inter-channel and inter-scan delay times were 0.02 and 0.10 s, respectively. The dwell time was 0.200 s for each analyte.

3. Results

3.1. *Shotgun proteome profiling by label-free nUPLC-MS^E*

We pursued a proteomic investigation to analyze the profile of proteins whose levels change in response to ATM expression in order to elucidate the role of ATM in the control of protein quality and stability. In the attempt to investigate the different protein profiling in presence of absence of ATM we focalized our study on two cell lines previously established [17]: lymphoblastoid ATM deficient cells from an A-T patient stably transfected with constructs that allow the expression of either FLAG-ATM-wt protein (L6-ATM-wt=L6ATM) or the empty vector as control (L6-pCDNA=L6). These two cell lines were obtained from the same lymphoblastoid clone; consequently they have the same genetic background and are specifically different only for the reconstitution of ATM expression. Therefore, the differences observed comparing these cell lines are reasonably, mainly due to the different expression of ATM protein. L6 and L6ATM cells were incubated 2 hours in the presence or in the absence of the proteasome inhibitor MG132 10 μM (Fig. 1). Two different datasets were analyzed: on the one hand a comparison between the proteome of L6ATM cell line and L6 cells (L6ATM *vs* L6); on the other hand a parallel between MG132 treated L6ATM cell line and MG132 treated L6 cells (L6ATM MG132 *vs* L6 MG132). The first dataset allowed us to investigate the differences in proteome composition only due to the presence/absence of ATM. The treatment with MG132 [41] allowed to highlight those proteins whose half-life is particularly short and their ATM dependent modulation levels over the whole proteome would be partially masked in a direct investigation. The comparative proteome analysis was performed by nano ultra performance liquid chromatography (nUPLC) coupled to MS^E isotope free shotgun profiling. Using this approach, we identified a total of 123153 molecular spectral features (EMRTs) and 473 proteins across both conditions of the first dataset (L6ATM *vs* L6); 119759 EMRTs and 503 proteins in the second dataset (L6ATM MG132 *vs* L6 MG132). Quality control measures were performed on the replicates to determine the mass measurement and the chromatographic retention time analytical reproducibility of each peptide (Fig. S1). The subsequent strategy for quantifying proteome profile data for differential expression analysis relies on changes in the peptide analyte signal response from each EMRT component that directly reflect their concentrations in one sample relative to another. Applying this experimental approach the label-free shotgun analysis of the two cell lines revealed that L6ATM cells showed significantly different levels of 53 proteins compared to L6 (Tables 1, S1–S7). The proteomic analysis of the second dataset under study (MG132 treated L6ATM *vs* MG132 treated L6 cells) led us to identify 62 proteins differentially expressed (Tables 2, S1, S8-S13). Among these identified proteins 12 were present in both comparison condition (see Tables 1 and 2).

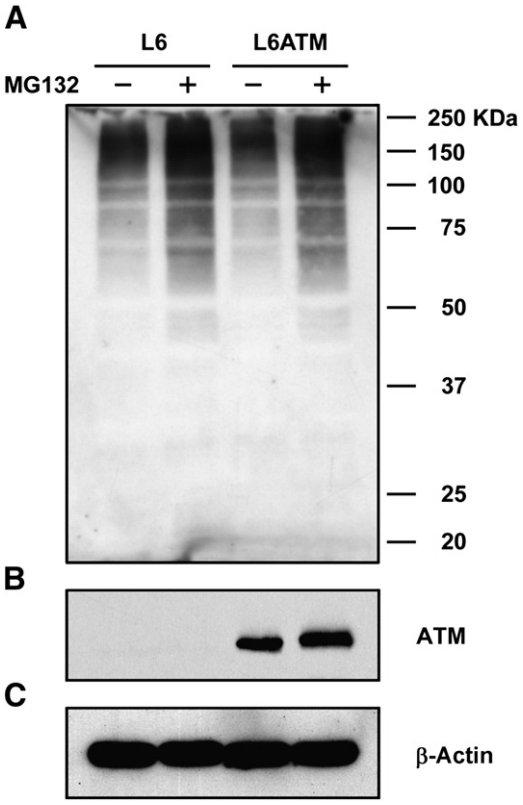

Fig. 1 – Assessment of proteasome inhibition. L6 and L6ATM cells treated 2 hours with 10 μM MG132 or DMSO 1:1000 (control). For immunoblotting, 50 μg protein extract were separated by SDS-PAGE and transferred on nitrocellulose. (A) Proteasome inhibition were confirmed by anti-Mono- and polyubiquitinylated conjugates (clone FK2) antibody. (B) ATM expression were assessed by anti-ATM western blot. (C) Equal protein loading was confirmed by β-Actin expression.

3.2. *Proteome-wide functional and pathway analysis*

Bioinformatics analysis was performed in order to analyze the functions of co-expressed genes and gain insight into the stressed process related to the absence of ATM activity. High-throughput experimental techniques, such as label-free proteomics analysis, produce large amounts of data but these data are of little use if it is not possible to interpret the results in a biological context. Therefore, we have analyzed our proteomics dataset by using two bioinformatic analysis tools, such as Protein Analysis Through Evolutionary Relationships (PANTHER) classification system and Ingenuity Pathways Analysis (IPA). Using the PANTHER resource we classified biologically relevant functional annotations of the differentially expressed polypeptides. The proteins identified in the two dataset of L6ATM *vs* L6 and L6ATM MG132 *vs* L6 MG132 were examined for their known GO biological process and grouped in the respective functional category. The most represented biological process (with 25% and 21% respectively) was linked to cellular metabolism (Fig. 2). To gain deeper insight into the plausible cellular and molecular networks in which the identified proteins might be involved, we used the two experimental dataset of L6ATM *vs* L6 and L6ATM MG132 *vs* L6 MG132 regulated dependent gene products to query IPA. In fact, Ingenuity Pathway Core Analysis reveals assessment of the enriched signaling and metabolic pathways, molecular networks, and biological processes that are most significantly perturbed in the dataset of interest. This unbiased systems biology approach identified significant over-representation of proteins involved in Glycolysis/gluconeogenesis canonical pathway for both comparison, respectively *p*-value = $3.34E^{-07}$ and *p*-value = $6.68E^{-07}$. These results are based on the ATM dependent differentially expression of some glycolytic/gluconeogenetic enzymes: Enolase 2 (gamma, neuronal), Glyceraldehyde-3–phosphate dehydrogenase, Glucose-6–phosphate isomerase, Phosphoglycerate mutase 1 (brain) (PGAM1), Phosphoglycerate kinase 1 (PGK1), Pyruvate kinase isozymes M1 M2 (PKM2). Moreover, in both dataset (L6ATM *vs* L6 and L6ATMMG132 *vs* L6MG132) among the top affected Molecular and Cellular Functions is the Carbohydrate Metabolism (*p*-value calculated for the first dataset: $7.11E^{-08}$ to $2.15E^{-02}$; for the second one: $6.34E^{-06}$ to $4.43E^{-02}$) (Tables 3 and S14).

3.3. *Protein expression and pathway analysis validation*

To validate our results, we selected one sub-set of proteins among those identified as differentially expressed by label-free shotgun experiments and checked their expression by means of western blot analysis performed on new cellular extracts (Fig. 3). The choice was made on the basis of the pathway analysis (selecting three enzyme: PGK1, PKM2 and PGAM1) and literature available information coherent with already published paper and/or with known ATM function (selecting other six proteins: hnRNPH, GLRX1, Plastin3, STAT1, LaminB and Matrin3. For detailed literature references see subsequent Result and Discussion section). Interestingly, we confirmed several data from other proteomic based studies (Table S15) [21–23,28,42] related to ATM and performed on other cell lines. A-T cells have a high level of genome instability, and there were likely numerous genetic changes before the wild type ATM protein was added back. The consistency of our experimental with those obtained by other cell lines enforced the collected results. . Moreover, in addition of both the L6 cell lines, we performed the western blot validation on two other cell lines, characterized by distinct genetic background: GM-03189 (lymphoblastoid cell line derived from an A-T patient) and a stable interfered for ATM HeLa cell line plus the relative control. All the proteins we analyzed both through proteomic and western blot analysis exhibited the same trend in up- or down-regulation of protein expression except for Matrin 3 (Fig. 3E, F). From proteomic analysis we noticed a high increment of Matrin 3 protein levels in L6 ATM treated with MG132; on the contrary protein levels analyzed by western blot seem to be lower. This contradictory result highlights again a well-known technical issue on differences between the two different types of experimental methods we adopted (nLC-MS/MS and western blot analysis); we could explain this discrepancy pondering over the inherent errors and limits of each technique and on the quality of commercial antibodies. Moreover, the down-regulation of Plastin 3 in absence of ATM was confirmed by means of western blotting in the L6 cells but not in

Table 1 – Significant differentially regulated proteins in L6ATM and L6 cells comparison identified by label-free LC-MS[E].

Accession[a]	Description (GN=gene name)	Score[b]	Highly represented[c]	L6ATM: L6 Ratio	L6ATM: L6 Log(e) Ratio	L6ATM:L6 Log(e) StdDev
P14174	Macrophage migration inhibitory factor GN=MIF	7075.59	L6ATM			
P53999	Activated RNA polymerase II transcriptional coactivator p15 GN=SUB1	2139.7	L6ATM			
Q32P51	Heterogeneous nuclear ribonucleoprotein A1 like 2 GN=HNRNPA1L2	1504.35	L6ATM			
P01876	**Ig alpha 1 chain C region GN=IGHA1**	1479.68	L6ATM			
P39687	Acidic leucine rich nuclear phosphoprotein 32 family member A GN=ANP32A	1443.88	L6ATM			
P35268	60 S ribosomal protein L22 GN=RPL22	681.5	L6ATM			
O14979	Heterogeneous nuclear ribonucleoprotein D like GN=HNRPDL	633.7	L6ATM			
P55795	Heterogeneous nuclear ribonucleoprotein H2 GN=HNRNPH2	445.99	L6ATM			
O60812	Heterogeneous nuclear ribonucleoprotein C like 1 GN=HNRNPCL1	413.2	L6ATM			
Q15181	Inorganic pyrophosphatase GN=PPA1	376.52	L6ATM			
P07954	Fumarate hydratase mitochondrial GN=FH	325.39	L6ATM			
Q16658	Fascin GN=FSCN1	319.98	L6ATM			
P12956	X ray repair cross complementing protein 6 GN=XRCC6	256.08	L6ATM			
A6NHL2	**Tubulin alpha chain like 3 GN=TUBAL3**	173.35	L6ATM			
P17844	Probable ATP dependent RNA helicase DDX5 GN=DDX5	147.85	L6ATM			
P52272	**Heterogeneous nuclear ribonucleoprotein M GN=HNRNPM**	129.17	L6ATM			
Q9Y4L1	Hypoxia up regulated protein 1 GN=HYOU1	115.98	L6ATM			
P46940	Ras GTPase activating like protein IQGAP1 GN=IQGAP1	112.27	L6ATM			
P13797	Plastin 3 GN=PLS3	473.76		7.03	1.95	0.38
Q99867	Putative tubulin beta 4q chain GN=TUBB4Q	787.96		4.44	1.49	0.2
P06454	Prothymosin alpha GN=PTMA	8347.55		2.36	0.86	0.09
Q15233	Non POU domain containing octamer binding protein GN=NONO	467.49		2.14	0.76	0.13
P07910	Heterogeneous nuclear ribonucleoproteins C1 C2 GN=HNRNPC	934.28		1.8	0.59	0.08
P00558	Phosphoglycerate kinase 1 GN=PGK1	546.96		1.73	0.55	0.05
P31947	14 3 3 protein sigma GN=SFN	751.6		1.67	0.51	0.51
P14618	Pyruvate kinase isozymes M1 M2 GN=PKM2	3573.08		1.58	0.46	0.03
P31943	Heterogeneous nuclear ribonucleoprotein H GN=HNRNPH1	251.07		1.48	0.39	0.1
P30101	**Protein disulfide isomerase A3 GN=PDIA3**	306.45		1.48	0.39	0.07
P19338	Nucleolin GN=NCL	323.14		1.45	0.37	0.08
P04406	Glyceraldehyde 3 phosphate dehydrogenase GN=GAPDH	21300.61		1.39	0.33	0.03
P18669	Phosphoglycerate mutase 1 GN=PGAM1	3870.24		1.35	0.3	0.06
P27348	14 3 3 protein theta GN=YWHAQ	2381.94		0.73	−0.32	0.17
Q13509	Tubulin beta 3 chain GN=TUBB3	5054.55		0.72	−0.33	0.16
P54652	Heat shock related 70 kDa protein 2 GN=HSPA2	1879.25		0.72	−0.33	0.25
P13929	Beta enolase GN=ENO3	1278.2		0.71	−0.34	0.3
P31146	**Coronin 1A GN=CORO1A**	4864.42		0.66	−0.42	0.05
P14866	Heterogeneous nuclear ribonucleoprotein L GN=HNRNPL	373.99		0.64	−0.45	0.13
P35579	**Myosin 9 GN=MYH9**	484.58		0.63	−0.47	0.05
Q562R1	**Beta actin like protein 2 GN=ACTBL2**	5361.02		0.59	−0.53	0.04
P08107	Heat shock 70 kDa protein 1A 1B GN=HSPA1A	813.92		0.48	−0.73	0.23
Q14974	Importin subunit beta 1 GN=KPNB1	636.75		0.4	−0.91	0.12
Q9Y281	Cofilin 2 GN=CFL2	5716.25		0.36	−1.01	0.26
Q6ZMR3	L lactate dehydrogenase A like 6A GN=LDHAL6A	446.94		0.26	−1.36	0.58
Q04917	**14 3 3 protein eta GN=YWHAH**	802.25		0.24	−1.43	0.21
P34931	**Heat shock 70 kDa protein 1 like GN=HSPA1L**	840.22		0.11	−2.22	0.35
P26641	Elongation factor 1 gamma GN=EEF1G	255.88	L6			
P20591	Interferon induced GTP binding protein Mx1 GN=MX1	265.5	L6			
P07602	Proactivator polypeptide GN=PSAP	331.8	L6			
P61158	Actin related protein 3 GN=ACTR3	425.19	L6			
P23381	**Tryptophanyl tRNA synthetase cytoplasmic GN=WARS**	690.49	L6			
P35754	Glutaredoxin 1 GN=GLRX	1109.59	L6			
P13284	Gamma interferon inducible lysosomal thiol reductase GN=IFI30	1124.13	L6			
P09211	Glutathione S transferase P GN=GSTP1	3276.57	L6			

(continued on next page)

GM-03189 cells (Fig. 3A, B), probably due to different genetic background and phenotypic adaptation among the two lymphoblastoid cell lines.

Western blot validation of the overexpression of three proteins belonging to the glycolysis pathway (PGK1, PGAM1 and PKM2, see Fig. 3A, B) and the interesting bioinformatics outcome strongly supports the idea that there is a modulation of the glycolytic metabolism in absence of ATM activity. To better qualify this potential metabolic shunt we decided to assess the related metabolic changes by HPLC-MS/MS analysis. In fact, it is not possible only with the performed bioinformatics analysis (GO protein annotation inferred by PANTHER and enrichment function and pathway analysis by IPA) to qualify if the identified process are down-regulated or up-regulated between samples; both bioinformatics tools are based only on the experimental proteins number (and not on their up- or down-regulation) under study by comparing the annotation terms outcome to the reference background (whole annotated functions). Five metabolites were evaluate monitoring their mass spectrometry transitions: glucose 6–phosphate (G 6–P), fructose 1,6–bisphosphate (F 1,6–P), glyceraldehyde 3–phosphate (G 3–P), pyruvate (P) and lactate (L) (Fig. 4). Levels of G 6–P, F 1,6–P and G 3–P intermediate glycolytic metabolites were higher in absence of ATM. On the contrary, levels of the end products of glycolysis (pyruvate) (approximately 1.5-fold increase), and lactate (approximately 3-fold increase) were higher in agreement with the higher expression level of PKM2 in ATM reconstituted L6 compared with the native L6 ATM deficient cell line. PKM2 is the rate-limiting enzyme of the glycolysis and catalyzes the transphosphorylation from phosphoenolpyruvate (PEP) to ADP as the last step of glycolysis to generate ATP and pyruvate. Hu et al. described an up-regulation of Pyruvate kinase isozymes M1 M2 (PKM2) in ATCL8 cells (expressing a functional ATM) compared with AT5BIVA (fibroblast cell line derived from a patient with A-T) due to 3 hours of irradiation [42]. Moreover, in another of proteomic study previously indicated, the authors isolated PKM2 through a large-scale proteomic analysis of proteins phosphorylated in response to DNA damage on consensus sites recognized by ATM and ATR [23]. Intriguingly is known in literature a nuclear translocation of PKM2 in response to different apoptotic stimuli and this nuclear translocation is sufficient to induce programmed cell death [43]. Our results and the reported published evidences confirm the hypothesis that PKM2 could be considered as one of the ATM target protein. Nevertheless, we observed an up-regulation of PKM2 in L6 ATM reconstituted cell line only in basal condition and not after the MG132 treatment. We can hypothesize that in the absence of ATM this protein is more degraded by the Ub-proteasome system and after the proteasome blockage there is an accumulation of the ubiquitylated protein in both cell line explaining the absence of different expression between the two treated cell lines in our study.

The last monitored metabolite, lactate, was found more concentrated in presence of ATM (approximately 3-fold increase in basal condition and 2-fold increase after MG132 treatment, Fig. 4) according to the higher amount of its precursor pyruvate. Normally, lactate is produced in mammalian organism when the oxygen availability is decreased in a reduction reaction that produces NAD^+ from NADH and H^+. In our cellular system we hypothesize that the lactate higher amount depends on its functions as thermodynamic driving force to push the glycolytic step of the Glyceraldehyde 3 phosphate dehydrogenase (GAPDH) which is enzymatically acting in near equilibrium condition.

4. Discussion

Ataxia Telangiectasia (A-T) is a genetic disease characterized by cerebellar ataxia and immunodeficiency. A-T is linked to the loss of ATM protein function, a serine/threonine kinase central in DNA damage response. ATM modulates also the activity of E3-ubiquitin-ligases, affecting the stability of target proteins. Therefore, ATM deficiency may severely impinge on the cellular proteome composition resulting in defective signaling pathways. In fact, there are increasing evidence that this protein may have an important role in the control of target proteins of the ubiquitin system. Stagni and colleagues have recently shown that ATM modulates the proteasome dependent down-regulation of c-FLIP [17,18]. In the present study, we have pursued a comprehensive proteomic investigation to evaluate the biological effects of ATM expression on the control of protein quality and stability. To this aim, protein expression profiling were also assessed in the presence of the proteasome inhibitor MG132 to highlight those proteins whose expression is modulated by ATM most likely through the ubiquitin–proteasome system and whose half-life is particularly short and their ATM dependent modulation levels over the whole proteome would be partially masked in a direct investigation. By label-free nLC-MS^E approach, a total of 53 and 62 differentially expressed proteins were identified in the two analyzed comparison (L6ATM *vs* L6ATM and MG132 treated L6ATM *vs* MG132 treated L6 cell lines, respectively). Twelve proteins are regulated in the same way in both experimental dataset and we can speculate that their expression is influenced by the presence/absence of ATM but this event occurs independently of the ubiquitin–proteasome system involvement. Remarkably one of them, Plastin 3 (PLS3), differentially regulated in both dataset of the shotgun proteomic experiments (overepressed in L6ATM cell line in presence or absence of MG132, Tables 1 and 2, Fig. 3A, B), is already known as phosphorylated upon DNA damage, probably by ATM or ATR

Notes to Table 1:
a: Unique protein sequence identifier according to UniProtKB/Swiss-Prot Protein Knowledgebase, release 2011_06.
b: ProteinLynx Global Server score.
c: Protein found highly represented in L6ATM or in L6 cells (ratio >20 or <0.05 respectively).
d: Ratio of expression between L6ATM and L6.
Boldface type indicates proteins identified as differentially regulated and with the same trend also in the MG132 treated L6ATM *vs* L6 comparison.
Proteins confirmed by way of western blotting are underlined.
Details of proteins and peptides identification are reported in Supporting Information.

Table 2 – Significant differentially regulated proteins in L6ATM MG132 and L6 MG132 treated cells identified by label-free LC-MS^E.

Accession[a]	Description (GN=gene name)	Score[b]	Highly represented[c]	L6ATM MG132: L6 MG132 ratio[d]	L6ATM MG132: L6 MG132 Log(e) ratio	L6ATM MG132: L6 MG132 Log(e) StdDev
Q9H853	Putative tubulin like protein alpha 4B GN=TUBA4B	3538.69	L6ATM MG132			
P01876	**Ig alpha 1 chain C region GN=IGHA1**	2023.93	L6ATM MG132			
P60660	Myosin light polypeptide 6 GN=MYL6	1832.83	L6ATM MG132			
P01903	HLA class II histocompatibility antigen DR alpha chain GN=HLA DRA	1273.34	L6ATM MG132			
P00441	Superoxide dismutase Cu Zn GN=SOD1	872.16	L6ATM MG132			
Q15365	Poly rC binding protein 1 GN=PCBP1	395.32	L6ATM MG132			
Q14240	Eukaryotic initiation factor 4A II GN=EIF4A2	394.71	L6ATM MG132			
P33316	Deoxyuridine 5 triphosphate nucleotidohydrolase mitochondrial GN=DUT	377.73	L6ATM MG132			
P23284	Peptidyl prolyl cis trans isomerase B GN=PPIB	347.71	L6ATM MG132			
P52272	**Heterogeneous nuclear ribonucleoprotein M GN=HNRNPM**	247.63	L6ATM MG132			
P29692	Elongation factor 1 delta GN=EEF1D	206.91	L6ATM MG132			
P11586	C 1 tetrahydrofolate synthase cytoplasmic GN=MTHFD1	165.9	L6ATM MG132			
P43243	Matrin 3 GN=MATR3	155.67	L6ATM MG132			
A6NHL2	**Tubulin alpha chain like 3 GN=TUBAL3**	150.41	L6ATM MG132			
Q16352	Alpha internexin GN=INA	150.09	L6ATM MG132			
P17661	Desmin GN=DES	123.55	L6ATM MG132			
Q08211	ATP dependent RNA helicase A GN=DHX9	120.64	L6ATM MG132			
P07197	Neurofilament medium polypeptide GN=NEFM	114.22	L6ATM MG132			
Q3ZCM7	Tubulin beta 8 chain GN=TUBB8	3060.88		4.48	1.5	0.24
P13797	**Plastin 3 GN=PLS3**	269.63		3.35	1.21	0.81
P09104	Gamma enolase GN=ENO2	1059.15		2.48	0.91	0.49
Q9H4B7	Tubulin beta 1 chain GN=TUBB1	724.79		2.34	0.85	0.19
P00558	**Phosphoglycerate kinase 1 GN=PGK1**	978.15		1.63	0.49	0.07
P30101	**Protein disulfide isomerase A3 GN=PDIA3**	420.89		1.43	0.36	0.05
P06744	Glucose 6 phosphate isomerase GN=GPI	231.58		1.39	0.33	0.09
Q00839	Heterogeneous nuclear ribonucleoprotein U GN=HNRNPU	184.59		1.39	0.33	0.06
P14625	Endoplasmin GN=HSP90B1	599.41		0.72	−0.33	0.05
Q15084	Protein disulfide isomerase A6 GN=PDIA6	489.55		0.71	−0.34	0.07
Q01518	Adenylyl cyclase associated protein 1 GN=CAP1	256.75		0.71	−0.34	0.14
P08133	Annexin A6 GN=ANXA6	255.34		0.7	−0.35	0.18
P35579	**Myosin 9 GN=MYH9**	388.97		0.68	−0.39	0.05
Q562R1	**Beta actin like protein 2 GN=ACTBL2**	3295.43		0.68	−0.39	0.02
Q9UL46	Proteasome activator complex subunit 2 GN=PSME2	809.71		0.68	−0.38	0.08
P31946	14 3 3 protein beta alpha GN=YWHAB	12498.36		0.66	−0.41	0.09
Q07021	Complement component 1 Q subcomponent binding protein mitochondrial GN=C1QBP	343.71		0.64	−0.44	0.16
P31146	**Coronin 1A GN=CORO1A**	3535.44		0.63	−0.47	0.04
P08865	40 S ribosomal protein SA GN=RPSA	1296.7		0.55	−0.6	0.07
P34931	**Heat shock 70 kDa protein 1 like GN=HSPA1L**	1371.37		0.55	−0.6	0.17
P20700	Lamin B1 GN=LMNB1	278.66		0.5	−0.7	0.12
Q58FG0	Putative heat shock protein HSP 90 alpha A5 GN=HSP90AA5P	452.22		0.44	−0.83	0.04
Q9BYX7	Putative beta actin like protein 3 GN=POTEKP	1963.52		0.41	−0.9	0.09

(continued on next page)

Table 2 *(continued)*

Accession[a]	Description (GN=gene name)	Score[b]	Highly represented[c]	L6ATM MG132: L6 MG132 ratio[d]	L6ATM MG132: L6 MG132 Log(e) ratio	L6ATM MG132: L6 MG132 Log(e) StdDev
P63104	14 3 3 protein zeta delta GN=YWHAZ	4893.36		0.41	−0.9	0.08
Q58FF7	Putative heat shock protein HSP 90 beta 3 GN=HSP90AB3P	1773.07		0.39	−0.95	0.17
Q9BUF5	Tubulin beta 6 chain GN=TUBB6	3586.51		0.36	−1.02	0.26
Q04917	**14 3 3 protein eta GN=YWHAH**	1239.37		0.36	−1.01	0.21
P07205	Phosphoglycerate kinase 2 GN=PGK2	286.5		0.24	−1.44	0.34
Q5TZA2	Rootletin GN=CROCC	48.78	L6 MG132			
P42224	Signal transducer and activator of transcription 1 alpha beta GN=STAT1	123.72	L6 MG132			
P50990	T complex protein 1 subunit theta GN=CCT8	126.06	L6 MG132			
Q9P1U1	Actin related protein 3B GN=ACTR3B	136.44	L6 MG132			
O15144	Actin related protein 2 3 complex subunit 2 GN=ARPC2	139.01	L6 MG132			
Q7KZF4	Staphylococcal nuclease domain containing protein 1 GN=SND1	139.62	L6 MG132			
Q15029	116 kDa U5 small nuclear ribonucleoprotein component GN=EFTUD2	146.71	L6 MG132			
P29401	Transketolase GN=TKT	168.37	L6 MG132			
O14556	Glyceraldehyde 3 phosphate dehydrogenase testis specific GN=GAPDHS	242.53	L6 MG132			
P23381	**Tryptophanyl tRNA synthetase cytoplasmic GN=WARS**	315.47	L6 MG132			
P52815	39 S ribosomal protein L12 mitochondrial GN=MRPL12	334.73	L6 MG132			
P52565	Rho GDP dissociation inhibitor 1 GN=ARHGDIA	403.89	L6 MG132			
O75083	WD repeat containing protein 1 GN=WDR1	506.88	L6 MG132			
Q99714	3 hydroxyacyl CoA dehydrogenase type 2 GN=HSD17B10	599.37	L6 MG132			
Q9P1F3	Costars family protein C6orf115 GN=C6orf115	879.52	L6 MG132			
P02042	Hemoglobin subunit delta GN=HBD	2211.94	L6 MG132			

a: Unique protein sequence identifier according to UniProtKB/Swiss-Prot Protein Knowledgebase, release 2011_06.
b: ProteinLynx Global Server score.
c: Protein found highly represented in L6ATM MG132 or L6 MG132 treated cells (ratio >20 or <0.05 respectively).
d: Ratio of expression between L6ATM MG132 and L6 MG132.
Boldface type indicates proteins identified as differentially regulated and with the same trend also in the L6ATM *vs* L6 comparison.
Proteins levels assessed by way of western blotting are underlined.

[23], and its levels are decreased in Spinal Muscular Atrophy (SMA, a neurological disease) mouse model [44].

We analyzed by western blot other three proteins whose levels were influenced by ATM expression and MG132 treatment: STAT1, Lamin B1 and Matrin 3 (Table 2, Fig. 3E, F) to confirm the regulation observed through proteomic analysis in both L6 treated cell lines. Signal Transducer and Activator of Transcription 1 (STAT1) has been previously identified as a potential substrate of ATM in nuclear extracts from irradiated (10 Gy) HeLa cells [21] enforcing the idea that this member of the STAT protein family could be a direct target of ATM. In our study STAT1 is down-regulated after proteasome blockage in L6 ATM compared to L6, an evidence that could be eventually explained by proteasome dependent degradation of STAT1 in ATM proficient cells. In response to cytokines and growth factors, STAT family members are phosphorylated by the receptor associated kinases, and then form dimers that translocate to the cell nucleus where they act as transcription activators of a variety of genes, which is thought to be important for cell viability in response to different cell stimuli and pathogens [45]. There are some evidences in literature which shine a light on the interplay between ATM and STAT1 in the response to the DNA damage, that strengthen our findings [46,47].

Moreover, we observed a decrease of Lamin B1(LMNB1) in L6 ATM treated cells; recently Barascu and colleagues demonstrated an upregulation of Lamin B1 in A-T cells extract. The authors stressed the point that LMNB1 overexpression is sufficient to induce nuclear shape alterations and senescence in wild-type cells. A-T patients suffer from premature ageing and this observation led to the hypothesis that Lamin B1 dysregulation could account for senescence in A-T cells [48]. The authors related LMNB1 accumulation to A-T associated DDR defects,

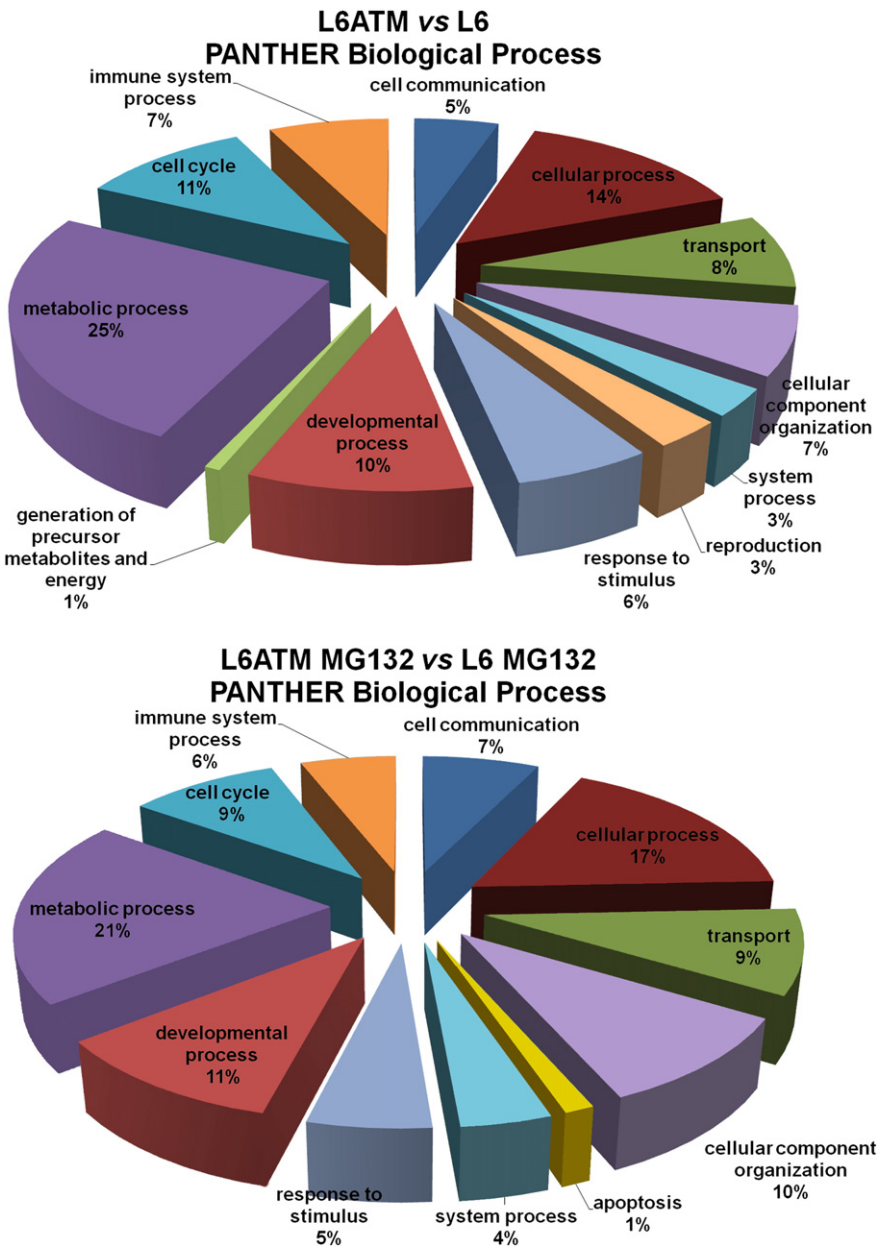

Fig. 2 – PANTHER biological process classification. Pie chart of Gene Ontology distribution terms associated to differentially regulated proteins.

oxidative stress and nuclear shape alterations. Finally, by a systematic analysis of human protein complexes to identify chromosome segregation proteins, ATM and LMNB1 were found as bait-prey interactors from affinity-purification - mass spectrometry experiments (www.mitocheck.org) [49]; this experimental evidence adds an interesting discussion point for the possible direct interaction between ATM and LMNB1 occurring in the nuclear compartment while the highly ordered processes of chromosome segregation and cell division is ongoing. Chromosome alignment, movement and segregation during cell division involve interactions between the kinetochore and the mitotic spindle through microtubule depolymerization/assembly [50]. Notably, we revealed differential expression of tubulins and Heat Shock Proteins (HSPs) in both proteomics dataset. Although the expression of some cytoskeleton proteins and HSPs could be related to their abundance and therefore to their more easily accessible identification by mass spectrometry experiments, in our opinion the selective presence of centrosome components, like tubulins, and Hsp 70 and 90 in our cell models is tied to their function in cell cycle control, cell death and aggresome promoting formation as described in several literature papers and already observed in our previous work [51]. Mediators of stress response (i.e., Checkpoint kinase 2 and its upstream regulator ATM) indeed regulate centrosome inactivation checkpoint and use stress inducted centrosome fragmentation or amplification for eliminating damaged cells [52]. The role of HSPs in cell cycle control and in signal transduction networks has been indeed described and assigned both to Hsp 90 [53] and Hsp 70. In particular Hsp 70, as binding partners of hSNM1B/Apollo, a protein with stimulating effect on ATM substrate

Table 3 – Ingenuity pathway analysis: top five canonical pathway and molecular and cellular function.

L6ATM *vs* L6	
Canonical pathways	***p*-Value**
Glycolysis/gluconeogenesis	3.34E−07
14-3-3-mediated signaling	1.51E−06
Cell cycle: G2/M DNA damage checkpoint regulation	3.41E−04
p70S6K Signaling	5.18E−04
Myc mediated apoptosis signaling	8.10E−04
Molecular and cellular functions	***p*-Value**
Carbohydrate metabolism	7.11E−08 to 2.15E−02
Cellular assembly and organization	9.45E−06 to 4.86E−02
RNA post-transcriptional modification	2.42E−05 to 4.56E−02
Drug metabolism	5.44E−05 to 2.76E−02
Cell death	5.65E−05 to 4.81E−02
L6ATM MG 132 *vs* L6 MG132	
Canonical pathways	***p*-Value**
14-3-3-mediated signaling	6.05E−09
Glycolysis/gluconeogenesis	6.68E−07
Cell cycle: G2/M DNA damage checkpoint regulation	4.77E−04
PI3K/AKT signaling	4.74E−04
p70S6K signaling	7.99E−04
Molecular and cellular functions	***p*-Value**
Cellular assembly and organization	3.3E−06 to 4.82E−02
Cellular function and maintenance	3.3E−06 to 4.76E−02
Carbohydrate metabolism	6.34E−06 to 4.43E−02
Protein synthesis	7.7E−05 to 3.09E−02
Cell morphology	1.18E−04 to 4.76E−02

phosphorylation in response to DNA-damage, results indirectly implicated in the maintenance of genome stability [54]. Recent studies have also disclosed the involvement of Hsp 70 in the preservation of cytoarchitecture. Zhang X. and colleagues have indeed described the "unexpected role" of Hsp 70 in promoting aggresome formation through the interaction with the cochaperone ubiquitin ligase Carboxyl terminal of Hsp70/Hsp90 interacting protein (CHIP) [55]. In conclusion the participation of tubulins and HSPs in cell surveillance mechanisms qualified them as additional implementing checkpoints recruited and activated by stress stimuli, thereby explaining in part their differentially expressed levels in ATM absence in our proteomic observations.

Among the proteins whose levels were influenced by ATM expression and MG132 treatment and were analyzed by western blot, Matrin 3 (MATR3) has already been identified as cross-reacting protein to phospho-specific antibodies against known ATM/ATR substrates [21]. Moreover, Matrin 3 has been already described in literature as involved in early stage of DSB response [56]. In fact, treatment with the radiomimetic agent neocarzinostatin and MATR3 depletion led to abnormal accumulation of cells at the S-phase of the cell cycle. We observed an up-regulated protein expression in L6ATM treated cells by nLC-MSE approach. On the other hand, we could not confirm these data through western blot analysis, thus we could not completely rely on the proteomic evidence.

Therefore, as first conclusion we can argue that our experimental data pointed out some stimulating proteins whose expression changes depending on ATM in presence of proteasome inhibition and could be considered potential ATM activity substrate through the Ub–P system: the transcription activator STAT1 and Lamin B1.

The second interesting point of discussion concerns the significant overrepresentation of proteins involved in glycolysis/gluconeogenesis pathway and carbohydrate metabolism molecular function supporting the idea that there is an evident switch of the metabolism, and in particular of the carbohydrate process, in absence of the ATM expression. Our observations showed how expression of ATM in L6 cells drives higher expression of glycolytic enzymes (PGK1, PGAM1 and PKM2), lower intermediate glycolytic metabolites and higher pyruvate production probably by a stimulation of the cellular rate of glycolysis. The higher lactate amounts may depend consequently both on higher levels of its precursor (pyruvate) and on its function as NADH depleting compound in order to avoid the blockage of glycolysis due to the GAPDH enzymatic step which is operated in near equilibrium condition. These findings are related with the emerging role of ATM as central regulator of cellular metabolism in response to oxidative stress, linking genome stability, cell cycle and carbon catabolism [57–60]. ATM is largely nuclear, acting as modulator of the cellular response to genotoxic stress and indeed our observed up-regulation of hnRNPH in ATM cells could possibly be related to its function in maintaining the genome integrity. In fact, hnRNPH has been described as part of a rescue mechanism of p53 mRNA 3′-end processing regulation in DNA-damaged cells [61]. Moreover, there are increasing evidences that ATM deficiency is not only cause of damage response lack of function; ATM localizes predominantly in the cytoplasm in neuronal and neuron-like cells [62,63] and cytoplasmatic ATM activity is involved in insulin signaling pathways [30,32]). Cosentino et al. [33] demonstrated the link between ATM and the pentose phosphate pathway (PPP) by inducing Glucose-6-phosphate dehydrogenase (G6PD) activity. G6PD is the limiting enzyme of the PPP metabolic pathway which in turn is responsible for the production of the essential antioxidant NADPH cofactor and nucleotide synthesis required to promote DSB repair. Acting as a sensor of reactive oxygen species (ROS), ATM could possibly shift the carbohydrate metabolism from glycolysis to the oxidative PPP under stress condition like DSBs. Shifting the energy source glucose-6–phosphate from glycolysis to PPP, the energy stored in carbohydrate backbones molecules will be shifted toward NADPH production and nucleotide synthesis instead of ATP and NADH produced by glycolysis. In our study we hypothesize a shift of the glycolytic pathway itself in ATM activity absence which may be due to an impairment in the functional link between glycolysis and mitochondrial metabolism. In a recent published paper [36], Mongiardi et al. demonstrated that ATM defective cells have an

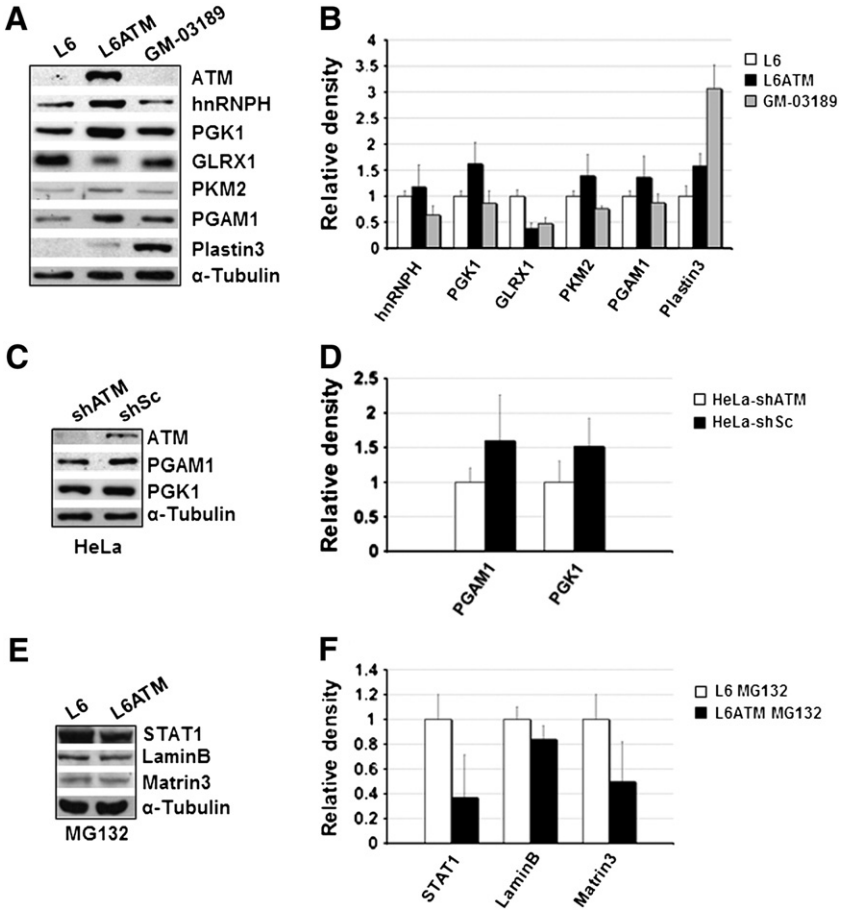

Fig. 3 – Immunoblotting validation of shotgun proteomic analysis. (A) Proteins levels revealed with specific antibodies in cellular extracts from L6 and L6ATM cells and a different human A-T lymphoblastoid (GM-03189) cell line characterized by distinct genetic background. Representative blots from three independent experiments with similar results are shown. Controls of equal protein loading were confirmed by α-Tubulin expression (mAb recognizing different isoforms other than ones identified by proteomic analysis). (B) Density of specific bands was measured by the image analysis software: ImageQuant TL; the level of each protein detected in A, has been normalized on the corresponding amount of α-Tubulin. The results are shown as the mean of the three independent experiments, and error bars represent standard deviation. (C) Proteins expression levels were analyzed also in HeLa cells interfered (shATM) or not (scramble, shSc) for ATM expression. Representative blots from three independent experiments with similar results are shown. (D) The level of each protein has been quantified and normalized as in B. The results are shown as the mean of the three independent experiments as in B. (E) Proteins levels detected in L6 and L6ATM cells after proteasome blockage. (F) The level of each protein has been quantified and normalized as in B. The results are shown as the mean of the three independent experiments as in B.

impaired mitochondrial activity, a reduced response to hypoxia in terms of HIF-1α stabilization and transcription of Hypoxia-responsive genes, including PGK1 and MIF. Accordingly, we identified these two gene products as down-regulated in L6 cells respect to L6ATM. The proposed explanation relays on a blunted response to hypoxia and intracellular concentration of ROS in response to hypoxia which in turn is due to an impaired sensing of oxygen variation. On the other end, in our study, the observed up-regulation of GLRX1 in ATM deficient cells could possibly be related to an adaptive response to mitigate the challenge of redox unbalance in ATM absence, a continuous stress state leading to genomic instability, accumulation of unrepaired DNA, constant activation of the DNA repair mechanisms and impaired mitochondrial activity. The transcription factor NF- κB, which has a pivotal role in cell survival and proliferation, is subject to regulation by redox changes; this regulation relies in part on the oxidative inactivation by means of S-glutathionylation of the Inhibitory κB kinase (IKK) β-subunit of the IKK signalosome; overexpression of GLRX1 catalyzes deglutathionylation of IKKβ and enhances NF-κB activation [64]. This evidence, our observation of GLRX1 up-regulation in ATM absence and the ATM dependent NEMO ubiquitylation and NF-κB activation [19] could possibly open a new route to an interesting vision on the linkage between ATM, NF-κB, genotoxic and oxidative stress, and cellular metabolism.

The present study provides initial evidences toward a new scenario of ATM function in cellular homeostasis; we are aware of the necessity to go deep inside this issue to complete the schema of signaling pathways beyond the differences in the metabolism response correlated to the loss of function of ATM. Nevertheless, all the described evidences begin to explain the intricate scenario beyond the A-T syndrome which could be

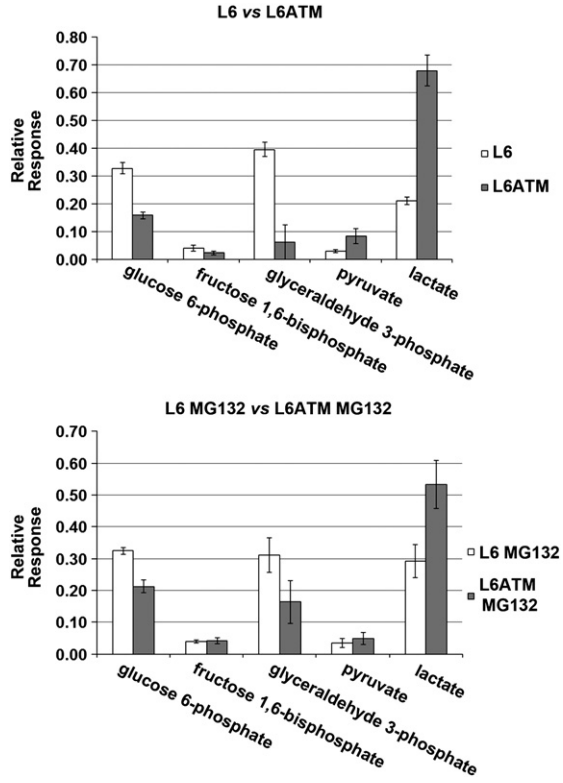

Fig. 4 – Metabolomics analysis. Metabolites were extracted from L6 and L6ATM cells in presence and absence of MG132. Levels of glucose 6–phosphate (G 6–P), fructose 1,6–bisphosphate (F 1,6–P), glyceraldehyde 3–phosphate (G 3–P), pyruvate (P) and lactate (L) in each extract were determined by mass spectrometry and reported as relative response (arbitrary units, calculated as the peak area of each analyte normalized to the total chromatographic peak areas). Error bars represent standard deviation calculated on three different analytical runs.

hardly understood as consequence only of the DNA damage response lack of function.

5. Conclusions

This research has led to the identification of a set of proteins whose levels and stability is modulated through ATM, therefore contributing to give insight into the molecular events of ATM deficiency relevant for neurodegeneration and immunodeficiency linked to A-T. Pattern of differentially expressed proteins in the presence and in the absence of ATM were obtained by shotgun label-free mass spectrometry characterization of lymphoblastoid ATM deficient and proficient cells. The treatment with MG132 highlights those proteins whose expression is modulated by ATM most likely through the ubiquitin–proteasome system and whose half-life is particularly short and their ATM dependent modulation levels over the whole proteome would be partially masked in a direct investigation. Our study pointed out some stimulating proteins whose expression changes could possibly depend on the ATM presence and the blockage of proteasome activity: Pyruvate kinase isozymes M1 M2, a glycolytic enzyme; Plastin 3, already known as involved neurological disease; the transcription activator STAT1 and Lamin B1. Moreover, proteomic and metabolomics data evidence a modulation of the carbohydrate metabolism in absence of ATM activity, in particular a different glycolysis rate. Our findings are related with the emerging role of ATM as central regulator of cellular carbohydrate metabolism in response to oxidative stress.

Supplementary data to this article can be found online at http://dx.doi.org/10.1016/j.jprot.2012.05.029.

Acknowledgements

This study was supported by Italian Telethon Foundation ("Comitato Telethon Fondazione Onlus", GGP07252 to D.B. and A.U.) and in part by the following grants: AIRC IG10590 to D.B. and Fondazione Roma 2008, "Rete Nazionale di Proteomica" FIRB RBRN07BMCT to A.U.

REFERENCES

[1] Lavin MF. Ataxia–telangiectasia: from a rare disorder to a paradigm for cell signalling and cancer. Nat Rev Mol Cell Biol 2008;9:759–69.
[2] Bhatti S, Kozlov S, Farooqi AA, Naqi A, Lavin M, Khanna KK. ATM protein kinase: the linchpin of cellular defenses to stress. Cell Mol Life Sci 2011;68:2977–3006.
[3] Shiloh Y. ATM and related protein kinases: safeguarding genome integrity. Nat Rev Cancer 2003;3:155–68.
[4] Gatti RA, Berkel I, Boder E, Braedt G, Charmley P, Concannon P, et al. Localization of an ataxia–telangiectasia gene to chromosome 11q22–23. Nature 1988;336:577–80.
[5] Savitsky K, Bar-Shira A, Gilad S, Rotman G, Ziv Y, Vanagaite L, et al. A single ataxia telangiectasia gene with a product similar to PI-3 kinase. Science 1995;268:1749–53.
[6] Bakkenist CJ, Kastan MB. DNA damage activates ATM through intermolecular autophosphorylation and dimer dissociation. Nature 2003;421:499–506.
[7] Hiom K. Coping with DNA double strand breaks. DNA Repair (Amst) 2010;9:1256–63.
[8] Messick TE, Greenberg RA. The ubiquitin landscape at DNA double-strand breaks. J Cell Biol 2009;187:319–26.
[9] Al-Hakim A, Escribano-Diaz C, Landry MC, O'Donnell L, Panier S, Szilard RK, et al. The ubiquitous role of ubiquitin in the DNA damage response. DNA Repair (Amst) 2010;9:1229–40.
[10] Dianov GL, Meisenberg C, Parsons JL. Regulation of DNA repair by ubiquitylation. Biochemistry (Mosc) 2011;76:69–79.
[11] Reinstein E, Ciechanover A. Narrative review: protein degradation and human diseases: the ubiquitin connection. Ann Intern Med 2006;145:676–84.
[12] Ciechanover A. Intracellular protein degradation: from a vague idea thru the lysosome and the ubiquitin–proteasome system and onto human diseases and drug targeting. Hematology Am Soc Hematol Educ Program 2006;1–12:505–6.
[13] Taylor A, Shang F, Nowell T, Galanty Y, Shiloh Y. Ubiquitination capabilities in response to neocarzinostatin and H(2)O(2) stress in cell lines from patients with ataxia–telangiectasia. Oncogene 2002;21:4363–73.
[14] Dornan D, Shimizu H, Mah A, Dudhela T, Eby M, O'Rourke K, et al. ATM engages autodegradation of the E3 ubiquitin ligase COP1 after DNA damage. Science 2006;313:1122–6.

[15] Khosravi R, Maya R, Gottlieb T, Oren M, Shiloh Y, Shkedy D. Rapid ATM-dependent phosphorylation of MDM2 precedes p53 accumulation in response to DNA damage. Proc Natl Acad Sci U S A 1999;96:14973–7.
[16] Maya R, Balass M, Kim ST, Shkedy D, Leal JF, Shifman O, et al. ATM-dependent phosphorylation of Mdm2 on serine 395: role in p53 activation by DNA damage. Genes Dev 2001;15:1067–77.
[17] Stagni V, di Bari MG, Cursi S, Condo I, Cencioni MT, Testi R, et al. ATM kinase activity modulates Fas sensitivity through the regulation of FLIP in lymphoid cells. Blood 2008;111: 829–37.
[18] Stagni V, Mingardi M, Santini S, Giaccari D, Barilà D. ATM kinase activity modulates cFLIP protein levels: potential interplay between DNA damage signalling and TRAIL-induced apoptosis. Carcinogenesis 2010;31:1956–63.
[19] Wu ZH, Shi Y, Tibbetts RS, Miyamoto S. Molecular linkage between the kinase ATM and NF-kappaB signaling in response to genotoxic stimuli. Science 2006;311:1141–6.
[20] Wood LM, Sankar S, Reed RE, Haas AL, Liu LF, McKinnon P, et al. A novel role for ATM in regulating proteasome-mediated protein degradation through suppression of the ISG15 conjugation pathway. PLoS One 2011;6: e16422.
[21] Mu JJ, Wang Y, Luo H, Leng M, Zhang J, Yang T, et al. A proteomic analysis of ataxia telangiectasia-mutated (ATM)/ATM-Rad3-related (ATR) substrates identifies the ubiquitin–proteasome system as a regulator for DNA damage checkpoints. J Biol Chem 2007;282:17330–4.
[22] Stokes MP, Rush J, Macneill J, Ren JM, Sprott K, Nardone J, et al. Profiling of UV-induced ATM/ATR signaling pathways. Proc Natl Acad Sci U S A 2007;104:19855–60.
[23] Matsuoka S, Ballif BA, Smogorzewska A, McDonald 3rd ER, Hurov KE, Luo J, et al. ATM and ATR substrate analysis reveals extensive protein networks responsive to DNA damage. Science 2007;316:1160–6.
[24] Ditch S, Paull TT. The ATM protein kinase and cellular redox signaling: beyond the DNA damage response. Trends Biochem Sci 2012;37:15–22.
[25] Kamsler A, Daily D, Hochman A, Stern N, Shiloh Y, Rotman G, et al. Increased oxidative stress in ataxia telangiectasia evidenced by alterations in redox state of brains from Atm-deficient mice. Cancer Res 2001;61:1849–54.
[26] Kuang X, Yan M, Ajmo JM, Scofield VL, Stoica G, Wong PK. Activation of AMP-activated protein kinase in cerebella of Atm–/– mice is attributable to accumulation of reactive oxygen species. Biochem Biophys Res Commun 2012;418: 267–72.
[27] Ambrose M, Goldstine JV, Gatti RA. Intrinsic mitochondrial dysfunction in ATM-deficient lymphoblastoid cells. Hum Mol Genet 2007;16:2154–64.
[28] Cheema AK, Timofeeva O, Varghese R, Dimtchev A, Shiekh K, Shulaev V, et al. Integrated analysis of ATM mediated gene and protein expression impacting cellular metabolism. J Proteome Res 2011;10:2651–7.
[29] Guo Z, Kozlov S, Lavin MF, Person MD, Paull TT. ATM activation by oxidative stress. Science 2010;330:517–21.
[30] Yang DQ, Kastan MB. Participation of ATM in insulin signalling through phosphorylation of eIF-4E-binding protein 1. Nat Cell Biol 2000;2:893–8.
[31] Peretz S, Jensen R, Baserga R, Glazer PM. ATM-dependent expression of the insulin-like growth factor-I receptor in a pathway regulating radiation response. Proc Natl Acad Sci U S A 2001;98:1676–81.
[32] Halaby MJ, Hibma JC, He J, Yang DQ. ATM protein kinase mediates full activation of Akt and regulates glucose transporter 4 translocation by insulin in muscle cells. Cell Signal 2008;20:1555–63.
[33] Cosentino C, Grieco D, Costanzo V. ATM activates the pentose phosphate pathway promoting anti-oxidant defence and DNA repair. EMBO J 2011;30:546–55.
[34] Shoelson SE. Banking on ATM as a new target in metabolic syndrome. Cell Metab 2006;4:337–8.
[35] Schneider JG, Finck BN, Ren J, Standley KN, Takagi M, Maclean KH, et al. ATM-dependent suppression of stress signaling reduces vascular disease in metabolic syndrome. Cell Metab 2006;4:377–89.
[36] Mongiardi MP, Stagni V, Natoli M, Giaccari D, D'Agnano I, Falchetti ML, et al. Oxygen sensing is impaired in ATM defective cells. Cell Cycle 2011;10.
[37] Silva JC, Gorenstein MV, Li GZ, Vissers JP, Geromanos SJ. Absolute quantification of proteins by LCMSE: a virtue of parallel MS acquisition. Mol Cell Proteomics 2006;5:144–56.
[38] Vissers JP, Langridge JI, Aerts JM. Analysis and quantification of diagnostic serum markers and protein signatures for Gaucher disease. Mol Cell Proteomics 2007;6:755–66.
[39] D'Aguanno S, D'Alessandro A, Pieroni L, Roveri A, Zaccarin M, Marzano V, et al. New insights into neuroblastoma cisplatin resistance: a comparative proteomic and meta-mining investigation. J Proteome Res 2011;10:416–28.
[40] Mi H, Dong Q, Muruganujan A, Gaudet P, Lewis S, Thomas PD. PANTHER version 7: improved phylogenetic trees, orthologs and collaboration with the Gene Ontology Consortium. Nucleic Acids Res 2010;38:D204–10.
[41] Lee DH, Goldberg AL. Proteasome inhibitors: valuable new tools for cell biologists. Trends Cell Biol 1998;8:397–403.
[42] Hu ZZ, Huang H, Cheema A, Jung M, Dritschilo A, Wu CH. Integrated bioinformatics for radiation-induced pathway analysis from proteomics and microarray data. J Proteomics Bioinform 2008;1:47–60.
[43] Stetak A, Veress R, Ovadi J, Csermely P, Keri G, Ullrich A. Nuclear translocation of the tumor marker pyruvate kinase M2 induces programmed cell death. Cancer Res 2007;67: 1602–8.
[44] Bowerman M, Anderson CL, Beauvais A, Boyl PP, Witke W, Kothary R. SMN, profilin IIa and plastin 3: a link between the deregulation of actin dynamics and SMA pathogenesis. Mol Cell Neurosci 2009;42:66–74.
[45] Santos CI, Costa-Pereira AP. Signal transducers and activators of transcription-from cytokine signalling to cancer biology. Biochim Biophys Acta 2011;1816:38–49.
[46] Townsend PA, Cragg MS, Davidson SM, McCormick J, Barry S, Lawrence KM, et al. STAT-1 facilitates the ATM activated checkpoint pathway following DNA damage. J Cell Sci 2005;118:1629–39.
[47] Pizarro JG, Folch J, Vazquez De la Torre A, Verdaguer E, Junyent F, Jordan J, et al. Oxidative stress-induced DNA damage and cell cycle regulation in B65 dopaminergic cell line. Free Radic Res 2009;43:985–94.
[48] Barascu A, Le Chalony C, Pennarun G, Genet D, Imam N, Lopez B, et al. Oxidative stress induces an ATM-independent senescence pathway through p38 MAPK-mediated lamin B1 accumulation. EMBO J 2012;31:1080–94.
[49] Hutchins JR, Toyoda Y, Hegemann B, Poser I, Heriche JK, Sykora MM, et al. Systematic analysis of human protein complexes identifies chromosome segregation proteins. Science 2010;328:593–9.
[50] Wade RH. On and around microtubules: an overview. Mol Biotechnol 2009;43:177–91.
[51] D'Alessandro A, D'Aguanno S, Cencioni MT, Pieroni L, Diamantini A, Battistini L, et al. Protein repertoire impact of ubiquitin–proteasome system impairment: insight into the protective role of beta-estradiol. J Proteomics 2012;75: 1440–53.

[52] Loffler H, Lukas J, Bartek J, Kramer A. Structure meets function—centrosomes, genome maintenance and the DNA damage response. Exp Cell Res 2006;312:2633–40.
[53] Young JC, Moarefi I, Hartl FU. Hsp90: a specialized but essential protein-folding tool. J Cell Biol 2001;154:267–73.
[54] Anders M, Mattow J, Digweed M, Demuth I. Evidence for hSNM1B/Apollo functioning in the HSP70 mediated DNA damage response. Cell Cycle 2009;8:1725–32.
[55] Zhang X, Qian SB. Chaperone-mediated hierarchical control in targeting misfolded proteins to aggresomes. Mol Biol Cell 2011;22:3277–88.
[56] Salton M, Lerenthal Y, Wang SY, Chen DJ, Shiloh Y. Involvement of Matrin 3 and SFPQ/NONO in the DNA damage response. Cell Cycle 2010;9:1568–76.
[57] Bar RS, Levis WR, Rechler MM, Harrison LC, Siebert C, Podskalny J, et al. Extreme insulin resistance in ataxia telangiectasia: defect in affinity of insulin receptors. N Engl J Med 1978;298:1164–71.
[58] Kruger A, Ralser M. ATM is a redox sensor linking genome stability and carbon metabolism. Sci Signal 2011;4:pe17.
[59] Yang DQ, Halaby MJ, Li Y, Hibma JC, Burn P. Cytoplasmic ATM protein kinase: an emerging therapeutic target for diabetes, cancer and neuronal degeneration. Drug Discov Today 2011;16:332–8.
[60] Perry JJ, Tainer JA. All stressed out without ATM kinase. Sci Signal 2011;4:pe18.
[61] Decorsiere A, Cayrel A, Vagner S, Millevoi S. Essential role for the interaction between hnRNP H/F and a G quadruplex in maintaining p53 pre-mRNA 3′-end processing and function during DNA damage. Genes Dev 2011;25:220–5.
[62] Oka A, Takashima S. Expression of the ataxia–telangiectasia gene (ATM) product in human cerebellar neurons during development. Neurosci Lett 1998;252:195–8.
[63] Boehrs JK, He J, Halaby MJ, Yang DQ. Constitutive expression and cytoplasmic compartmentalization of ATM protein in differentiated human neuron-like SH-SY5Y cells. J Neurochem 2007;100:337–45.
[64] Reynaert NL, van der Vliet A, Guala AS, McGovern T, Hristova M, Pantano C, et al. Dynamic redox control of NF-kappaB through glutaredoxin-regulated S-glutathionylation of inhibitory kappaB kinase beta. Proc Natl Acad Sci U S A 2006;103:13086–91.